



HAL
open science

Volumetric and dimensional accuracy assessment of CAD-CAM–manufactured dental prostheses from different materials

William Pacquet, Laurent Tapie, Bernardin Mawussi, Philippe Boitelle

► To cite this version:

William Pacquet, Laurent Tapie, Bernardin Mawussi, Philippe Boitelle. Volumetric and dimensional accuracy assessment of CAD-CAM–manufactured dental prostheses from different materials. *Journal of Prosthetic Dentistry*, 2023, 129 (1), pp.150-159. <10.1016/j.prosdent.2021.05.024>. <hal-04075845>

HAL Id: hal-04075845

<https://hal.science/hal-04075845v1>

Submitted on 31 Mar 2025

HAL is a multi-disciplinary open access archive for the deposit and dissemination of scientific research documents, whether they are published or not. The documents may come from teaching and research institutions in France or abroad, or from public or private research centers.

L'archive ouverte pluridisciplinaire **HAL**, est destinée au dépôt et à la diffusion de documents scientifiques de niveau recherche, publiés ou non, émanant des établissements d'enseignement et de recherche français ou étrangers, des laboratoires publics ou privés.



Distributed under a Creative Commons CC BY-NC 4.0 - Attribution - Non-commercial use - International License

JPD-20-1351

RESEARCH AND EDUCATION

Volumetric and dimensional accuracy assessment of CAD-CAM manufactured dental prosthesis from different materials

William Pacquet, DDS, MS, PhD(c),^a Laurent Tapie, MS, PhD,^b Bernardin Mawussi, MS, PhD,^c and Philippe Boitelle, DDS, MS, PhD^d

^aAssistant professor, Oral rehabilitation Department, Faculty of Dentistry, University Lille Nord de France, Paris, France.

^bSenior Lecturer, Mechanical engineering Department, University Sorbonne Paris Nord, Paris, France.

^cProfessor and Senior Lecturer, Mechanical engineering Department, University Sorbonne Paris Nord, Paris, France.

^dSenior Lecturer, Oral rehabilitation Department, Faculty of Dentistry, University Lille Nord de France, Paris, France.

ABSTRACT

Statement of problem. In computer-aided design and computer-aided manufacturing (CAD-CAM) dentistry, the CAD of the prosthesis represents the clinical prerequisite design to restore the treated tooth. However, how closely the CAM prosthesis shape matches the CAD, particularly in relation to different materials, is unclear.

Purpose. The purpose of this in vitro study was to evaluate onlays designed and manufactured with the same CAD-CAM system but manufactured with different materials.

Material and methods. A single standard tessellation language (STL) model was used to produce 6 composite resin onlays, 6 leucite glass-ceramic onlays, and 6 lithium disilicate glass-ceramic onlays. The onlays were digitized by using an X-ray microtomographic protocol with a metrological calibration. The CAD model was then compared with the scans of the different onlays. An analysis by region of interest was then carried out to assess the accuracy and reliability of the dimensional accuracy.

Results. The composite resin and the lithium disilicate glass-ceramic had the best dimensional accuracy. The leucite glass-ceramic exhibited a lack of trueness linked to consistent overmilling. The composite resin had less peripheral chipping than the glass-ceramics.

Conclusions. The composite resin and the lithium disilicate glass-ceramic material exhibited satisfactory dimensional accuracy. Milling the glass-ceramic before crystallization considerably improved dimensional accuracy.

CLINICAL IMPLICATIONS

Different materials are available to manufacture dental prostheses with CAD-CAM systems, the most important parameters being the prosthesis dimensional accuracy. For example, internal and proximal surface undermilling may prevent prosthesis insertion or accurate margins, and overmilling may promote bonded joint degradation. Clinicians should choose machinable materials, composite resin, leucite glass-ceramic, or lithium disilicate glass-ceramic, according to their machinability.

Despite the popularity of computer-aided design and computer-aided manufacturing (CAD-CAM), studies on the ability of numerical control machine tools to accurately produce the designed prosthesis are lacking.¹ These digital systems should limit human bias and standardize the quality of fixed prostheses.^{2,3} However, despite advanced digital technology, the complex tooth preparation shapes can lead to failures.⁴

CAD-CAM materials are typically selected based on their clinical properties. For example, a ceramic material might be selected for its optical properties depending on the esthetic requirements, while a composite resin material will be preferred for its low abrasiveness depending on the occlusal relationship.^{2,5} However, the machinability of the material leading to minimal surface and volumetric defects has rarely been considered.⁶ Nevertheless, the brittle behavior of certain materials can affect clinical outcome,⁷⁻¹⁰ and studies are lacking on the effects of the machining process on prosthesis shape in relation to the material.¹¹

A prosthesis with poor dimensional accuracy results in poorly fitting intaglio or proximal surfaces. On the occlusal surface, adjustments may weaken the prosthesis. Poor intaglio adaptation may lead to degradation of the bonded interface.^{12,13}

The machinability of a CAD-CAM material has generally been evaluated by its surface roughness or marginal chipping.¹⁴⁻¹⁶ However, the overall concept of machinability must also reflect the ability of a CAM system to reproduce the requested CAD geometry. In the present study, the dimensional accuracy with respect to the CAD model was evaluated.¹⁷ The research hypothesis was that the CAD model and the digitized CAM would be identical. A comparison was made between a clinical reference prosthesis designed by CAD and the digitization of prostheses machined by the same CAM system from different materials.

MATERIAL AND METHODS

Following the metrological calibration step of the measurement chain, the prostheses were scanned by using X-ray microtomography and digitally processed to be numerically superimposed on the reference CAD model.¹⁸ Thus, the machinability of a composite resin material (Tetric CAD; Ivoclar Vivadent AG), a leucite glass-ceramic material (Empress CAD; Ivoclar Vivadent AG), and a lithium disilicate glass-ceramic material (e.max CAD; Ivoclar Vivadent AG) were compared. An Ivorine mandibular first molar in a dentate typodont (ANKA-4 ZE; Frasco GmbH) was prepared and used for all the prostheses compared in the study. The tooth was prepared with diamond rotary instruments according to current recommendations¹⁹⁻²⁶ (Set LD0424A; Komet) and finished with flexible abrasive disks (Clearfil twist dia; Kuraray). The onlay preparation was based on a 2-mm-deep primary cavity with proximal walls that diverged between 6 and 10 degrees. The mesiolingual cusp was covered^{20,23} with a chamfer margin, a design suitable for onlays without a high esthetic requirement.^{25,26}

The prepared tooth, its antagonist, and the occlusion were digitized with a laboratory scanner with a resolution of 5 μm (TRIOS D2000; 3Shape A/S). The restorations were designed by using a dental CAD software program (TRIOS Dental Designer, v19.3.0; 3Shape A/S). The standard tessellation language (STL) CAD model of the prosthesis became the shape reference in this protocol.

Eighteen onlays were milled with CAM by using a 5-axis numerically controlled machine tool for dental use (Programill PM7; Ivoclar Vivadent AG) with the milling parameters and associated machining strategy recommended by the manufacturer. For each of the 3 series of materials, the same 4 milling tools were used: a $\text{\O}3$ -mm round-end diamond rotary instrument at 42 000 rpm, a $\text{\O}2$ -mm round-end diamond rotary instrument at 42 000 rpm, a $\text{\O}1$ -mm round-end

diamond rotary instrument at 42 000 rpm, and a Ø0.5-mm pointed-end diamond rotary instrument at 48 000 rpm for the occlusal fossae. Each series was milled simultaneously, and the diamond rotary instruments were changed for each group. The machining strategy has been reported to have a major impact on the quality of the definitive prosthesis.²⁷⁻³² Six onlays were made in lithium disilicate glass-ceramic (e.max CAD; Ivoclar Vivadent AG), 6 in leucite glass-ceramic (Empress CAD; Ivoclar Vivadent AG), and 6 in composite resin (Tetric CAD; Ivoclar Vivadent AG). The attachment areas of the prostheses were not removed to eliminate human intervention.

A first calibration step allowed the validation of the measurement chain,¹⁸ which was applied to a grade 5 ceramic ball of known dimension and density. Once the error level was known and was considered reliable, the protocol was applied to all specimens. As the object was a sphere, a Gaussian sphere associated with the points cloud was numerically constructed by using the least-squares method. The digitized sphere form deviation was evaluated by the analysis of distances between the digitized object mesh and the Gaussian sphere determined by construction of the orthogonal projection.³³⁻³⁵ According to this calibration, the measurement error was estimated by 1-dimensional deviation and 1-form deviation criteria introduced by the measurement chain. Once these 2 criteria were 10 times below the clinically acceptable dimensional and formed deviation, the measurement chain was considered reliable.

The X-ray microtomographic acquisitions of the onlays were performed by using a microcomputed tomography (μ CT) X-ray microtomograph (Quantum FX; Perkin Elmer) with an accelerating voltage of 100 kV, an amperage of 100 mA, and a resolution of 20 μ m. After the X-ray microtomographic acquisitions, image processing, segmentation, and extraction were carried out by using a software program (Image J; National Institutes of Health). Gray level

segmentation was carried out on the images by using auto-thresholding with an isomorphic algorithm because the material was homogeneous and uniform. The image stacks were processed to obtain a 3D model in STL format. The resulting meshes were transferred to an inspection software program for metrological analysis of points cloud data (GOM Inspect 2018; (Gesellschaft für Optische Messtechnik GmbH). The inspection software program was categorized with the lowest measurement deviations (class 1) by the Physikalisch-Technische Bundesanstalt (PTB) and the National Institute of Standards and Technology (NIST).

The reference CAD point cloud represented by its STL model was superimposed on the STL model resulting from the X-ray microtomographic acquisition, and metrological inspections were carried out in 3-dimensional maps. The GOM inspect global best fit function was used for the superimposition of the CAD and the mesh to minimize all deviations between both nominal and actual surfaces because no datum structures allowed a local best fit. The 3-dimensional maps were carried out by the orthogonal projections of the CAD model mesh on the digitized onlay mesh. Four common regions of interest (ROI) were delimited on the CAD model in order to measure the same areas on each machined prosthesis: an occlusal area, a proximal area, the internal area, and the marginal limit. A quantitative evaluation was carried out by exporting the numerical values of the distances of each orthogonal projection for each ROI. The measurement values embedded in an American Standard Code for Information Interchange (ASCII) file were then postprocessed with a digital calculation software program (Scilab Enterprises). The values were then classified according to their frequencies to produce frequency diagrams and trend curves. The frequency of absent projections was considered in these diagrams under the name of “undefined” values. Accuracy was analyzed according to the International Organization for Standardization (ISO) standard 5725.³⁶⁻³⁷

RESULTS

Global 3D mapping of 1 representative specimen of each series is shown in Figure 1. The frequency diagrams of the orthogonal projection values of the CAD model on the digital prosthesis are shown in Figure 2 for the internal ROI, in Figure 3 for the occlusal area ROI, in Figure 4 for the proximal ROI, and in Figure 5 for the marginal limit ROI. The median values of the distances of the different ROI are presented in Table 1.

DISCUSSION

The CAD-CAM production of dental prostheses makes it theoretically possible to avoid many human biases and should make it possible to optimize production and reproducibility. Unfortunately, the accumulation of physical and digital dispersions within this entire CAD-CAM system induces a difference between the requested CAD model and the physical prosthesis produced.³⁸ The method used in this study allowed a reliable and reproducible quantitative numerical analysis concerning the difference between the requested CAD model and the physical prosthesis. The data supported rejecting the null hypothesis that the CAD model and the digitized CAM would be identical. However, the complexity of the shape of a dental prosthesis prevented a conventional presentation of results with means and standard deviations. Indeed, complex shapes cause different variations, whether material excess or deficiency, and deviation distribution did not follow a Gaussian distribution resulting in nonrepresentative means and large standard deviations. Dividing prostheses into ROI overcame this problem because an area with similar manufacturing constraints presented similar defects. Furthermore, it allowed a table of the defects in the form of frequency diagrams, which provide a significant description of the

defects of the same ROI. In addition, the ROI was divided by clinical interest, which allowed a clinical extrapolation of the type of defects.

The parameters associated with the machining strategies did not change depending on the material. However, optimization of the tool path has been reported to reduce peripheral chipping considerably.^{27,28} In addition, the rotational speed and feed rate and the grit size of the tools have a major impact on chipping.²⁹⁻³²

Global maps as seen in Figure 1 provide much information concerning the influence of the tool-material couple and the tool-shape couple on the machinability of prostheses. Overmilled areas or deficient areas appear in blue, while undermilled areas or excess areas appear in red. However, the red area on the lingual side of the prosthesis corresponded to the attachment point. This part was present in excess on the prosthesis because it was absent on the digital design and would be removed by the dental laboratory technician.

Concerning the general appearance of the prostheses, the Tetric CAD specimens appeared to be overall undersized, while the e.max CAD specimens appeared adequate and the Empress CAD specimens appeared oversized. This was consistent with the material-tool couple relative to the material; Tetric CAD is a composite resin with a higher wear rate than the 2 others. The Archard general wear equation explains the wear rate with the relative influence of various parameters including load, surface hardness, or tool roughness.¹⁶ The difference between Empress CAD and e.max CAD can be explained by the fact that e.max CAD is partially crystallized (in the form of a blue block) to facilitate milling.

From a more local point of view, the occlusal fossae of all prostheses were undermilled, which corresponded to a gap between the requirements of the requested CAD and the technical constraints of the CAM. In this case, this was the size of the smallest tool used, which was larger

in diameter than the size of the occlusal fossae. The difference between the occlusal fossae in the composite resin and in the fully crystallized glass-ceramic may have been because of the different material-tool couple. Finally, deep and fine anatomic grooves were produced by machining brittle materials at the risk of initiating cracks.^{7,8}

In the marginal limit ROI, the more brittle materials such as glass-ceramics were more subject to peripheral chipping under the machining loads, but more ductile materials such as composite resins were less affected.^{9,10} Furthermore, peripheral deficiencies were more apparent for the Empress CAD, which was already fully crystallized, unlike the e.max CAD, which was milled before crystallization. The median table, as seen in Table 1, confirms the difference between the marginal limit ROI of the e.max CAD and the Empress CAD. The glass-ceramic milled after crystallization was oversized compared with the 2 other materials.

Clinically, a marginal discrepancy of less than 80 μm has been considered undetectable.³⁵ The distances between +40 μm and -40 μm will be the satisfactory range, while values lower or higher than the limit of this interval could indicate errors in the CAD-CAM system. All the medians in Table 1 were included in the satisfactory range between +40 μm and -40 μm . The presentation of trend curves helps confirm the trueness and precision of machining based on ROI. Accuracy was defined according to the ISO 5725 standard as the combination of trueness and precision.^{23,24} Precision is the ability to give the same results for the same true value, resulting in a narrow trend curve. Trueness is the ability to give average results corresponding to the true value; this results in a peak of the curve centered on zero because this value corresponded to the absence of a difference between the 2 analyzed elements.

Regarding the internal ROI as seen in Figure 2, the Tetric CAD and e.max CAD trend curves were narrow and zero-centered with values within the satisfactory range (93.2% of values

within satisfactory range for Tetric CAD and 96.5% for the e.max CAD). The internal area milling of Tetric CAD and e.max CAD specimens was expected to be accurate. For the Empress CAD, the trend curve was not zero-centered and was more extended (77.1% of values within the satisfactory range), which reflected the undermilled aspect of the lower surface of Empress CAD. Clinically, this will lead to a prosthesis that will be difficult to insert and the potential need for internal manual adjustment, which may promote fractures, as well as increased marginal microleakage.^{7,8}

Regarding the occlusal ROI as seen in Figure 3, the Tetric CAD and e.max CAD trend curves were zero-centered, which confirms their accuracy. However, the frequencies of values were excessive, which confirms the lack of precision (68.3% of values within satisfactory range for the Tetric CAD and 66.6% for the e.max CAD). Lack of precision was mainly because of the significant presence of machining defects that were greater than the satisfactory range (25.1% for e.max CAD and 25.6% for Empress CAD); these areas of the occlusal fossae were inaccessible to the rotary instruments, reducing prosthesis accuracy. The Empress CAD trend curve was narrower (more precise) but too far from zero (49.8% of values within the satisfactory range), and the frequency of values greater than the satisfactory range represented 45.2% of the distribution of values. The occlusal surfaces of all groups were generally undermilled and excessively undermilled in the Empress CAD group. Clinically, undermilled occlusal grooves may lead to an imprecise occlusal relationship. Occlusal adjustment by the dental laboratory technician may initiate cracks.^{7,8}

Regarding the proximal ROI as seen in Figure 4, the Tetric CAD trend curve was narrow but not zero-centered, despite 89.5% of values within the satisfactory range. This was because 52.6% of the defects were between 0.02 mm and 0.04 mm, leading to overmilling of the

proximal area. The CAD e.max has a narrow zero-centered trend curve, with 89.7% of values in the satisfactory range. The reproduction of the proximal area in the e.max CAD was therefore accurate. For the Empress CAD, the proximal surface was also undermilled with 54.0% of values within the satisfactory range, 53.2% of which were between 0.02 mm and 0.04 mm; 35.8% of the values were above the satisfactory range. Clinically, an overmilled proximal surface will result in a deficient proximal contact, while an undermilled proximal surface will result in an excessive contact that will need to be adjusted on delivery.³⁹

Regarding the marginal limit ROI as seen in Figure 5, the trend curves of Tetric CAD and e.max CAD were extended and were not zero-centered (46.2% of values included in the confidence interval for Tetric CAD and 50.6% for e.max CAD). Values outside the satisfactory range were typically lower. Despite comparable numerical values, from the global maps of these areas as seen in Figure 6, these values reflect 2 phenomena: excessive thinning imposed by marginal thickness close to zero (mostly in composite resin) and marginal chipping (mostly in glass-ceramic). Extremely low thickness areas cannot be machined accurately, and brittle materials like glass-ceramic will fracture. For the Empress CAD, the curve shows 2 peaks and although 56.4% of the values were within the satisfactory range, this was because the overall undermilled aspect of the prosthesis compensated for these values.

The tables of marginal limit ROI present values that were considered undefined because these zones did not allow the distance created by the orthogonal projections from the digitized onlay mesh on the CAD model mesh. Excessive defects prevent the software program from finding a point to establish a distance by orthogonal projection, as seen in Figure 7. These values were therefore attributable to chipping and can be associated with values less than -0.10 mm; the sum of these values represents 2.3% for the Tetric CAD, 4.2% for the e.max Cad, and 10.6% for

the Empress CAD. The tools used were similar for each specimen, whereas the material-tool couple has a major impact on chipping.²⁶⁻²⁸ Chipping reduces marginal fit, bonding surface, and restoration lifetime, increases plaque retention, and can adversely affect esthetics.^{12,14} Volume quantification, as well as the design of the chips, would require future investigation.

CONCLUSIONS

Based on the findings of this in vitro study, the following conclusions were drawn:

1. Machining strategies such as tool paths, tool grid size, rotational speed, or feed rate were not adapted to the machinable material, within the same machine.
Furthermore, machining strategies were not adapted to clinical regions of interest.
2. The composite resin material (Tetric CAD) had a satisfactory dimensional accuracy despite a slight overmilling due to the material-tool couple. Moreover, the material exhibited the least peripheral chipping.
3. The leucite glass-ceramic material (Empress CAD) had low trueness with overall undermilling, the weakest accuracy, and the greater peripheral chipping, possibly because of the material hardness which was milled after final crystallization.
4. The lithium disilicate glass-ceramic material (e.max CAD) had satisfactory dimensional accuracy, similar to that of composite resin but with a higher level of chipping, possibly because the material was milled before final crystallization.

REFERENCES

1. Benic GI, Sailer I, Zeltner M, Gütermann JN, Özcan M, Mühlemann S. Randomized controlled clinical trial of digital and conventional workflows for the fabrication of zirconia-ceramic fixed partial dentures. Part III: Marginal and internal fit. *J Prosthet Dent* 2019;121:426-31.
2. Miyazaki T, Hotta Y, Kunii J, Kuriyama S, Tamaki Y. A review of dental CAD/CAM: current status and future perspectives from 20 years of experience. *Dent Mater J* 2009;28:44-56.
3. Li RWK, Chow TW, Matinlinna JP. Ceramic dental biomaterials and CAD/CAM technology: State of the art. *J Prosthodont Res* 2014;58:208-16.
4. Zimmermann M, Valcanaia A, Neiva G, Mehl A, Fasbinder D. Influence of different CAM strategies on the fit of partial crown restorations: A digital three-dimensional evaluation. *Oper Dent* 2018;43:530-8.
5. Ruse ND, Sadoun MJ. Resin-composite blocks for dental CAD/CAM applications. *J Dent Res* 2014;93:1232-4.
6. Lambert H, Durand J-C, Jacquot B, Fages M. Dental biomaterials for chairside CAD/CAM: State of the art. *J Adv Prosthodont* 2017;9:486-95.
7. Gonzaga CC, Cesar PF, Miranda WG, Yoshimura HN. Slow crack growth and reliability of dental ceramics. *Dent Mater Off Publ Acad Dent Mater* 2011;27:394-406.
8. Benaqqa C, Chevalier J, Saädaoui M, Fantozzi G. Slow crack growth behaviour of hydroxyapatite ceramics. *Biomaterials* 2005;26:6106-12.
9. Rossetti PHO, do Valle AL, de Carvalho RM, De Goes MF, Pegoraro LF. Correlation between margin fit and microleakage in complete crowns cemented with three luting agents. *J Appl Oral Sci Rev FOB* 2008;16:64-9.

10. Trajtenberg CP, Caram SJ, Kiat-amnuay S. Microleakage of all-ceramic crowns using self-etching resin luting agents. *Oper Dent* 2008;33:392-9.
11. Schaefer O, Kuepper H, Thompson GA, Cachovan G, Hefti AF, Guentsch A. Effect of CNC-milling on the marginal and internal fit of dental ceramics: A pilot study. *Dent Mater Off Publ Acad Dent Mater* 2013;29:851-8.
12. Dong XD, Ruse ND. Fatigue crack propagation path across the dentinoenamel junction complex in human teeth. *J Biomed Mater Res A* 2003;66:103-9.
13. Boitelle P, Mawussi B, Tapie L, Fromentin O. A systematic review of CAD/CAM fit restoration evaluations. *J Oral Rehabil* 2014 Nov;41:853-74.
14. Lebon N, Tapie L, Vennat E, Mawussi B. Influence of CAD/CAM tool and material on tool wear and roughness of dental prostheses after milling. *J Prosthet Dent* 2015;114:236-47.
15. Chavali R, Nejat AH, Lawson NC. Machinability of CAD-CAM materials. *J Prosthet Dent* 2017;118:194-9.
16. Palin WM, Fleming GJ, Burke FJ, Marquis PM, Pintado MR, Randall RC, et al. The frictional coefficients and associated wear resistance of novel low-shrink resin-based composites. *Dent Mater* 2005;21:1111-8.
17. Jeong Y-G, Lee W-S, Lee K-B. Accuracy evaluation of dental models manufactured by CAD/CAM milling method and 3D printing method. *J Adv Prosthodont* 2018;10:245-51.
18. Pacquet W, Tapie L, Mawussi B, Boitelle P. Evaluation of the dimensional accuracy of manufactured dental prosthesis in relation to its computer-aided model. *Int J Comput Dent* 2020;23:1-8.
19. Ahlers MO, Mörig G, Blunck U, Hajtó J, Pröbster L, Frankenberger R. Guidelines for the preparation of CAD/CAM ceramic inlays and partial crowns. *Int J Comput Dent* 2009;12:309-

25.

20. Guess PC, Schultheis S, Wolkewitz M, Zhang Y, Strub JR. Influence of preparation design and ceramic thicknesses on fracture resistance and failure modes of premolar partial coverage restorations. *J Prosthet Dent* 2013;110:264-73.

21. Holberg C, Rudzki-Janson I, Wichelhaus A, Winterhalder P. Ceramic inlays: Is the inlay thickness an important factor influencing the fracture risk? *J Dent* 2013;41:628-35.

22. Ferraris F. Posterior indirect adhesive restorations (PIAR): preparation designs and adhesthetics clinical protocol. *Int J Esthet Dent* 2017;12:482-502.

23. Chang Y-H, Lin W-H, Kuo W-C, Chang C-Y, Lin C-L. Mechanical interactions of cuspal-coverage designs and cement thickness in a cusp-replacing ceramic premolar restoration: A finite element study. *Med Biol Eng Comput* 2009;47:367-74.

24. Krifka S, Stangl M, Wiesbauer S, Hiller K-A, Schmalz G, Federlin M. Influence of different cusp coverage methods for the extension of ceramic inlays on marginal integrity and enamel crack formation in vitro. *Clin Oral Investig* 2009;13:333-41.

25. Veneziani M. Posterior indirect adhesive restorations: updated indications and the morphology driven preparation technique. *Int J Esthet Dent* 2017;12:204-30.

26. Rocca GT, Rizcalla N, Krejci I, Dietschi D. Evidence-based concepts and procedures for bonded inlays and onlays. Part II. Guidelines for cavity preparation and restoration fabrication. *Int J Esthet Dent* 2015;10:392-413.

27. Jahanmir S. Ultrahigh speed microgrinding of dental ceramics. *Mach Sci Technol* 2010;14:411-22.

28. Gaspar M, Weichert F. Integrated construction and simulation of tool paths for milling dental crowns and bridges. *Comput-Aided Des* 2013;45:1170-81.

29. Dong X, Yin L, Jahanmir S, Ives LK, Rekow ED. Abrasive machining of glass-ceramics with a dental handpiece. *Mach Sci Technol* 2000;4:209-33.
30. Song X-F, Yin L, Han Y-G, Li J. Finite element analysis of subsurface damage of ceramic prostheses in simulated intraoral dental resurfacing. *J Biomed Mater Res* 2008;85:50-9.
31. Song X-F, Yin L. Subsurface damage induced in dental resurfacing of a feldspar porcelain with coarse diamond burs. *J Biomech* 2009;42:355-60.
32. Yin L, Jahanmir S, Ives LK. Abrasive machining of porcelain and zirconia with a dental handpiece. *Wear* 2003;255:975-89.
33. Tapie L, Chiche N, Boitelle P and al. Adaptation Measurement of CAD/CAM dental crowns with x-ray micro-CT: Metrological chain standardization and 3D gap size distribution. *Adv Mater Sci Eng* 2016;2016:1-13.
34. Du LY, Umoh J, Nikolov HN, Pollmann SI, Lee T-Y, Holdsworth DW. A quality assurance phantom for the performance evaluation of volumetric micro-CT systems. *Phys Med Biol* 2007;52:7087.
35. Johnston SM, Johnson GA, Badea CT. Geometric calibration for a dual tube/detector micro-CT system. *Med Phys* 2008;35:1820-9.
36. International Organization for Standardization. Accuracy (trueness and precision) of measurement methods and results — Part 1 : General principles and definitions. ISO 1994.
37. International Organization for Standardization. Accuracy (trueness and precision) of measurement methods and results — Part 2 : Basic method for the determination of repeatability and reproducibility of a standard measurement method. ISO 2019.
38. Tapie L, Lebon N, Mawussi B, Fron Chabouis H, Duret F, Attal J-P. Understanding dental CAD/CAM for restorations--the digital workflow from a mechanical engineering viewpoint. *Int J*

Comput Dent 2015;18:21-44.

39. Newman MG. Newman and Carranza's clinical periodontology. 13th edition. Philadelphia, PA: Elsevier, Inc; 2018. p. 944.

Corresponding author:

Dr William Pacquet

Research Unit in Innovative Dental Materials and Interfaces (URB2i-UR 4462)

Université de Paris and Université Paris 13

1 rue M. Arnoux 92120 Montrouge

FRANCE

Email: pacquet.william@gmail.com

TABLE

Table 1. Median values of projections by ROI and material

Material	Internal ROI	Occlusal ROI	Proximal ROI	Marginal limit ROI
Tetric CAD	7.3 μm	17.8 μm	-25.5 μm	-39.8 μm
Empress CAD	31.0 μm	39.6 μm	36.5 μm	15.5 μm
e.max CAD	-8.0 μm	19.1 μm	-15.7 μm	-36.5 μm

CAD, computer-aided design; ROI, region of interest.

FIGURES

Figure 1. Three-dimensional global maps of one specimen of each group.

Figure 2. Frequency diagrams of distances (mm) of internal region of interest.

Figure 3. Frequency diagrams of distances (mm) of occlusal region of interest.

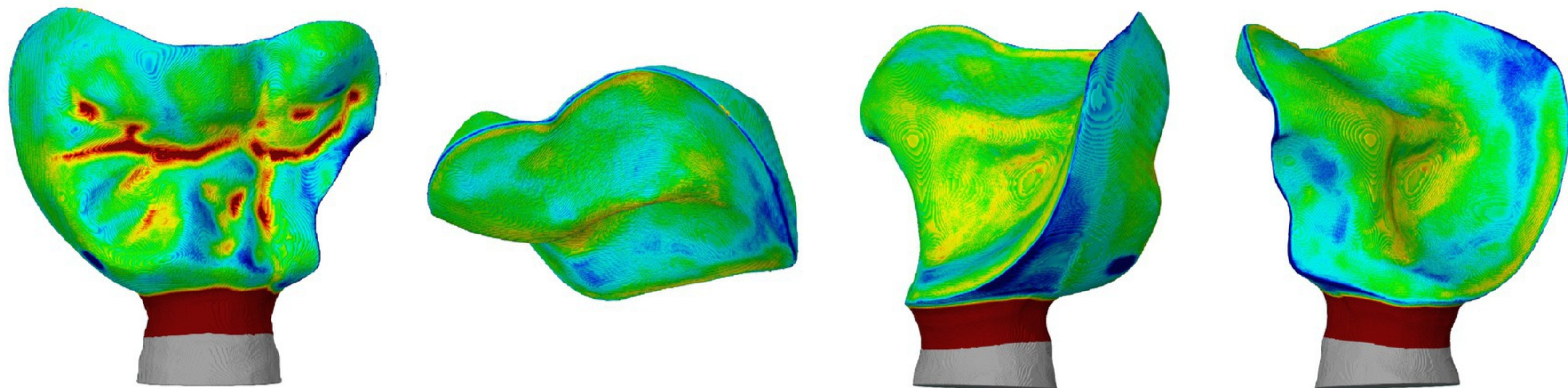
Figure 4. Frequency diagrams of distances (mm) of proximal region of interest.

Figure 5. Frequency diagrams of distances (mm) of marginal limit region of interest.

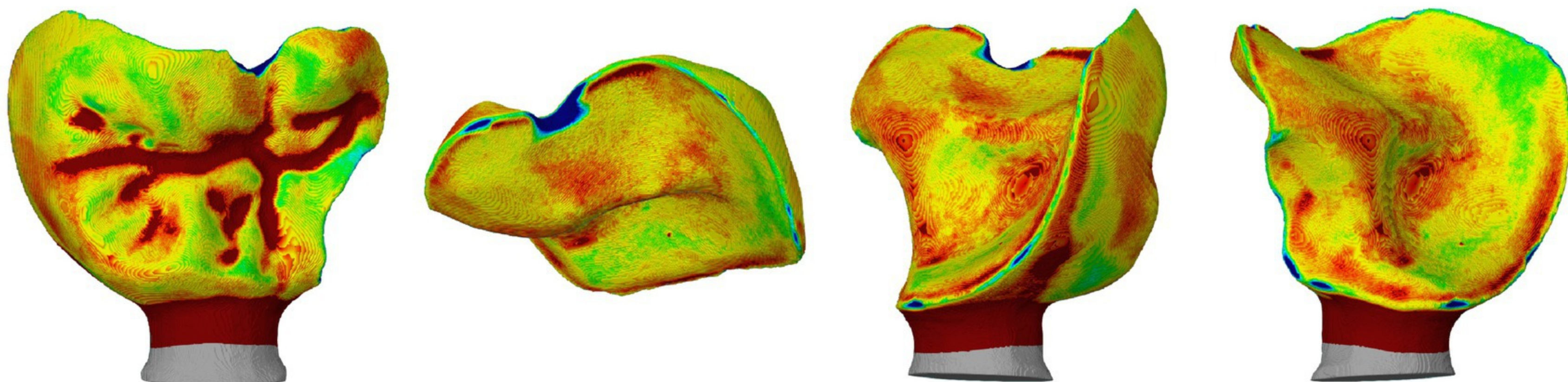
Figure 6. Comparison of marginal limit region of interest on specimen of Tetric CAD (*left*) and e.max CAD (*right*).

Figure 7. Map of peripheral region of interest projected on computer-aided design presenting one “undefined” defect at top and global mapping projected on mesh of corresponding prosthesis at bottom.

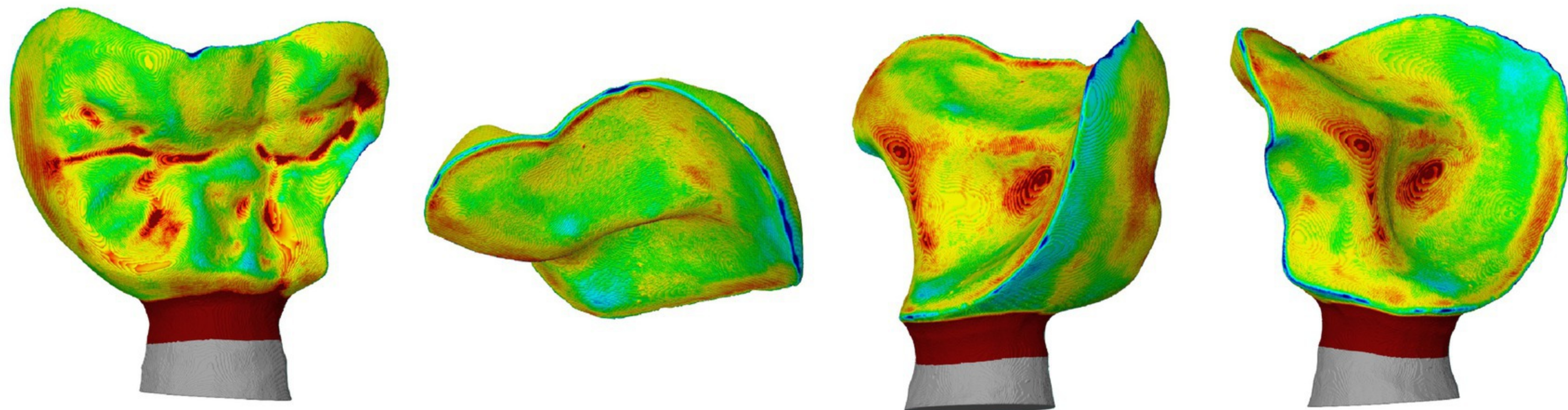
Tetric CAD



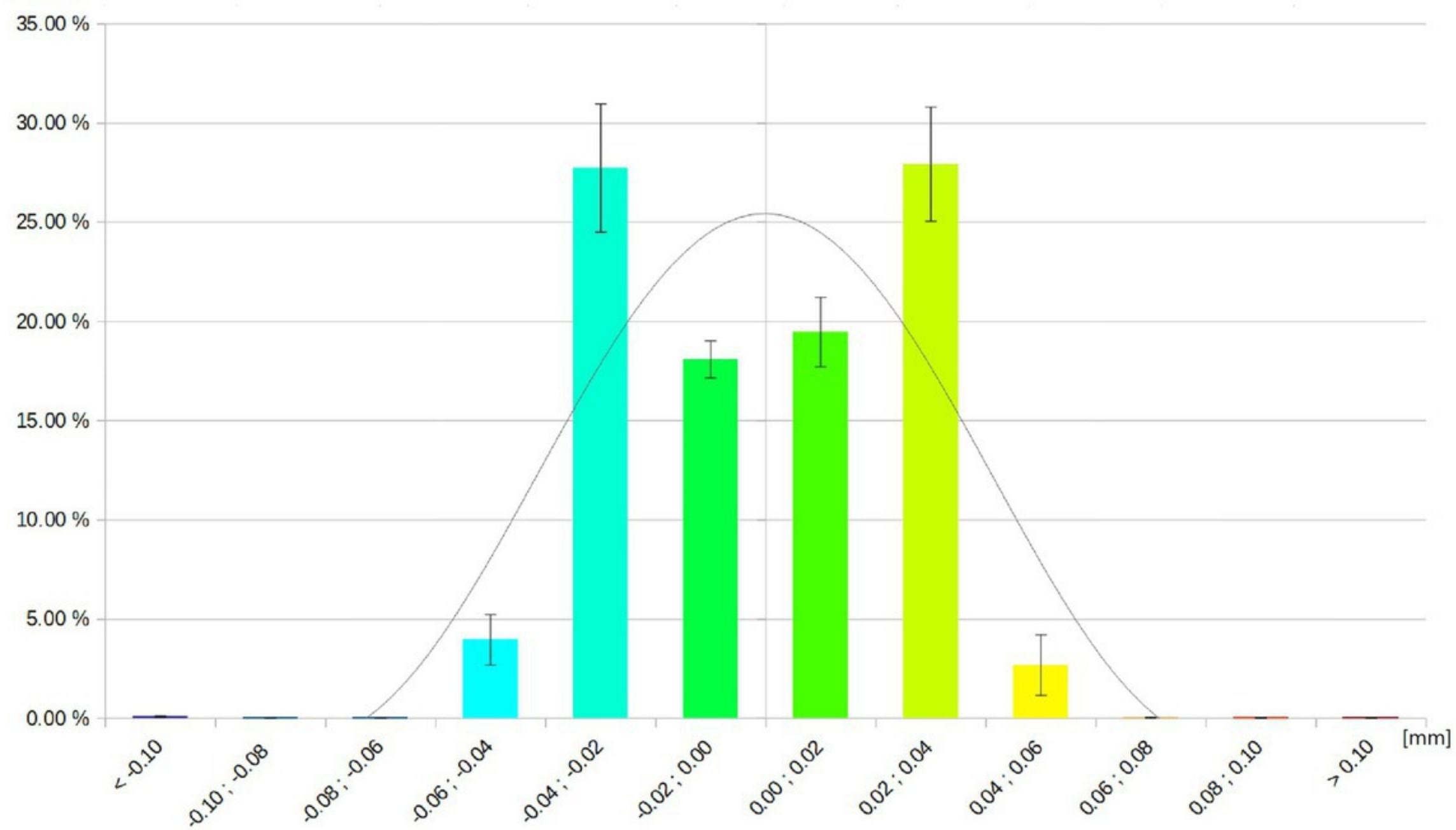
Empress CAD



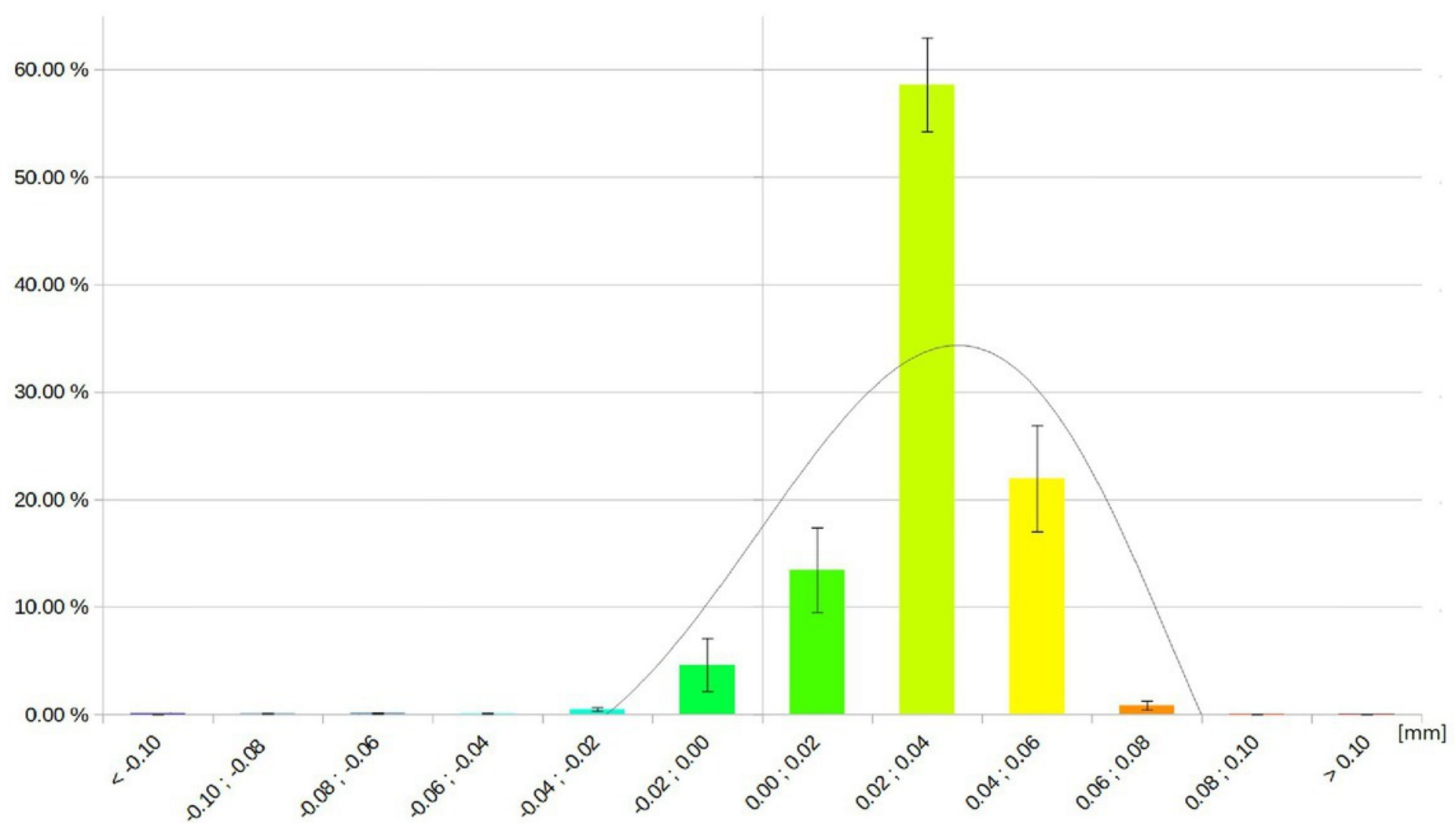
Emax CAD



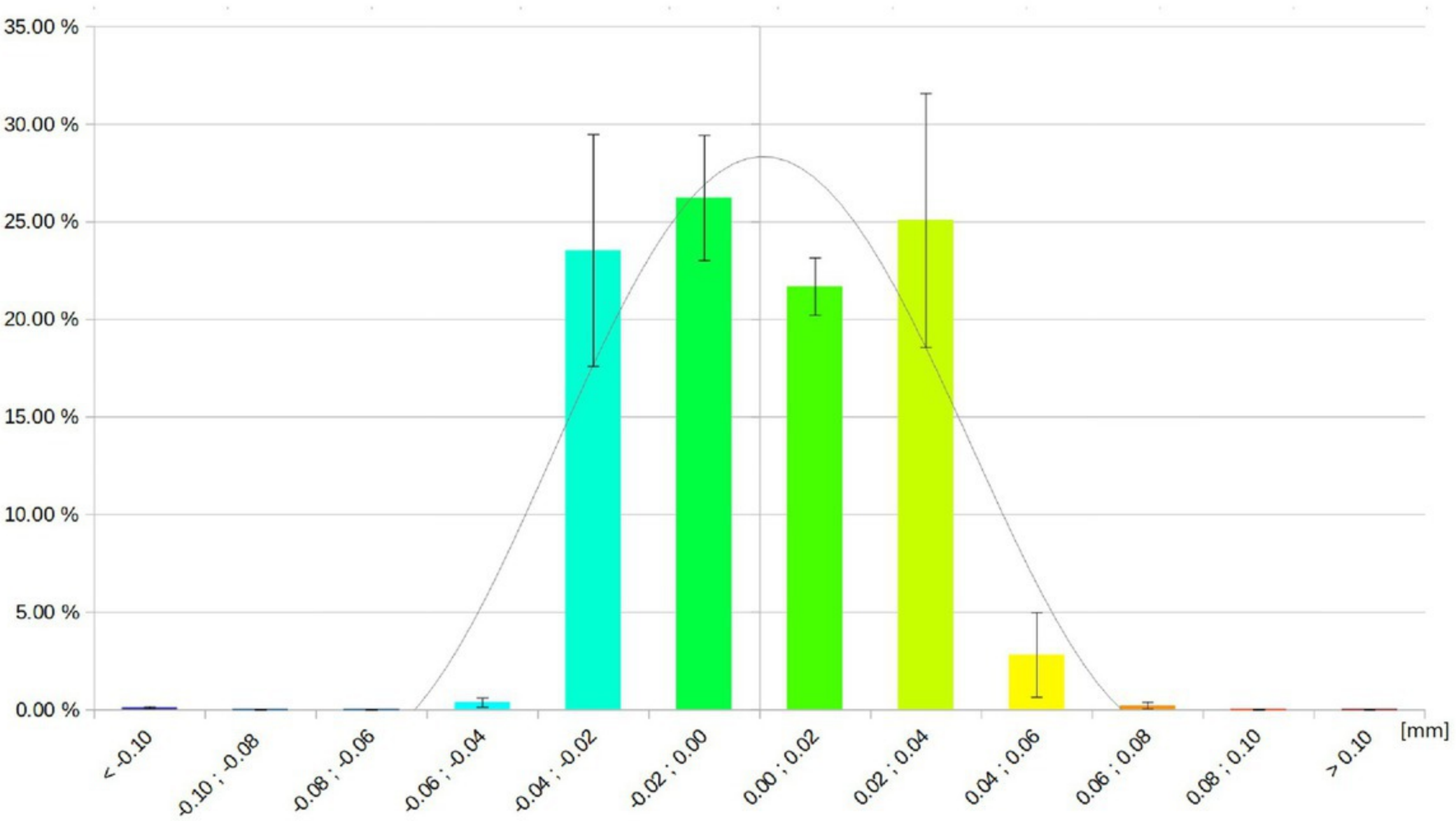
Tetric CAD



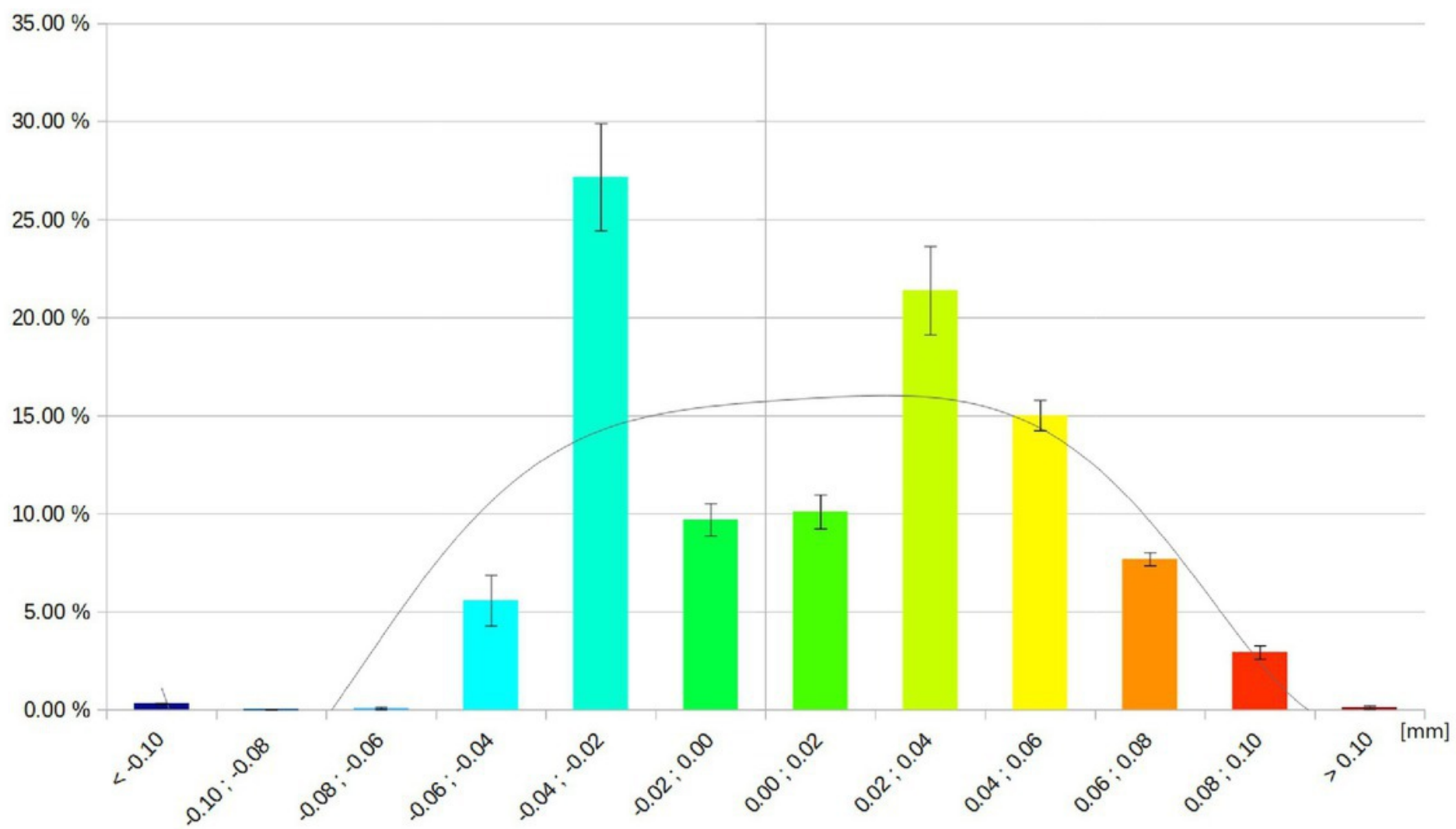
Empress CAD



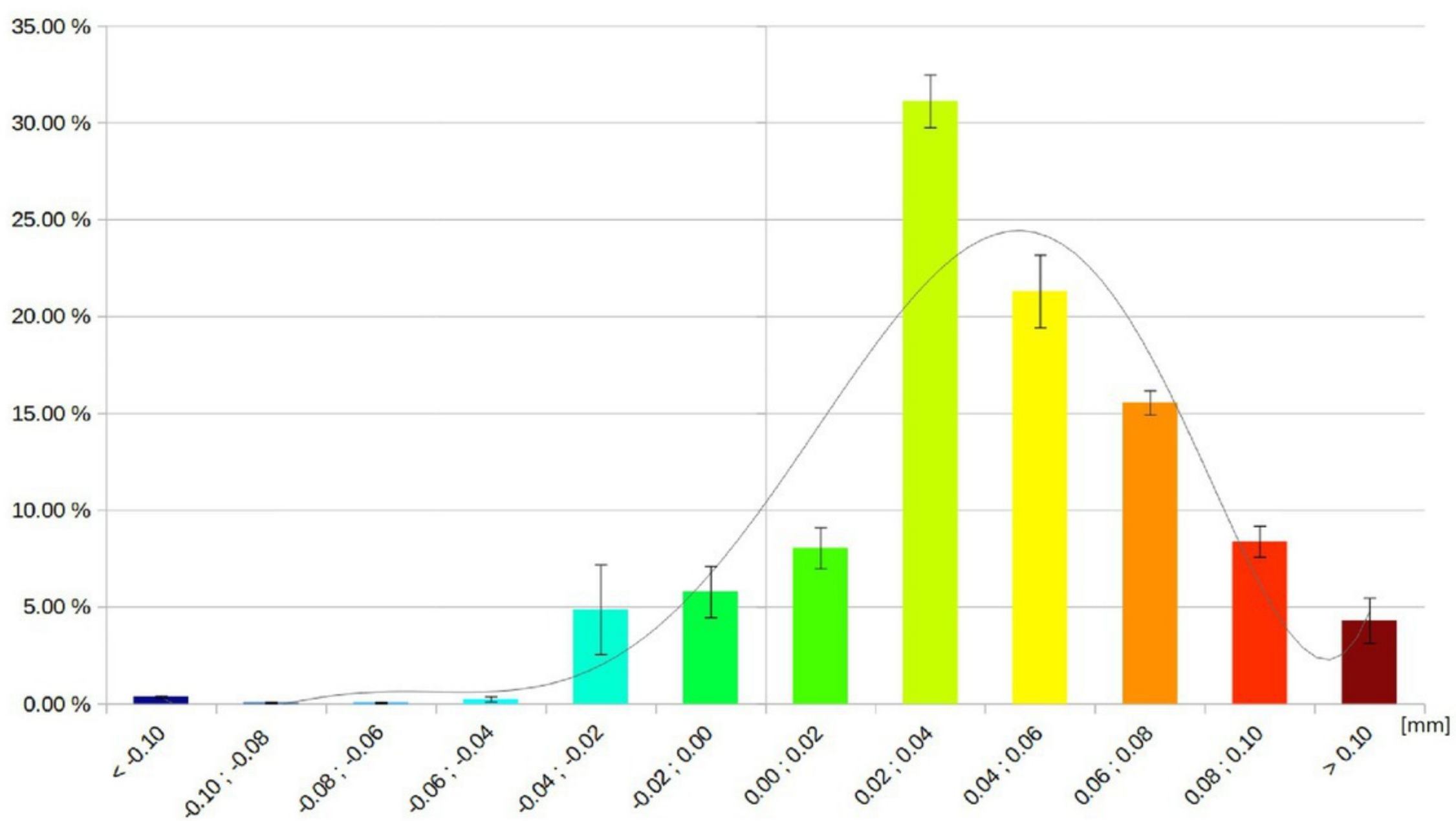
e.max CAD



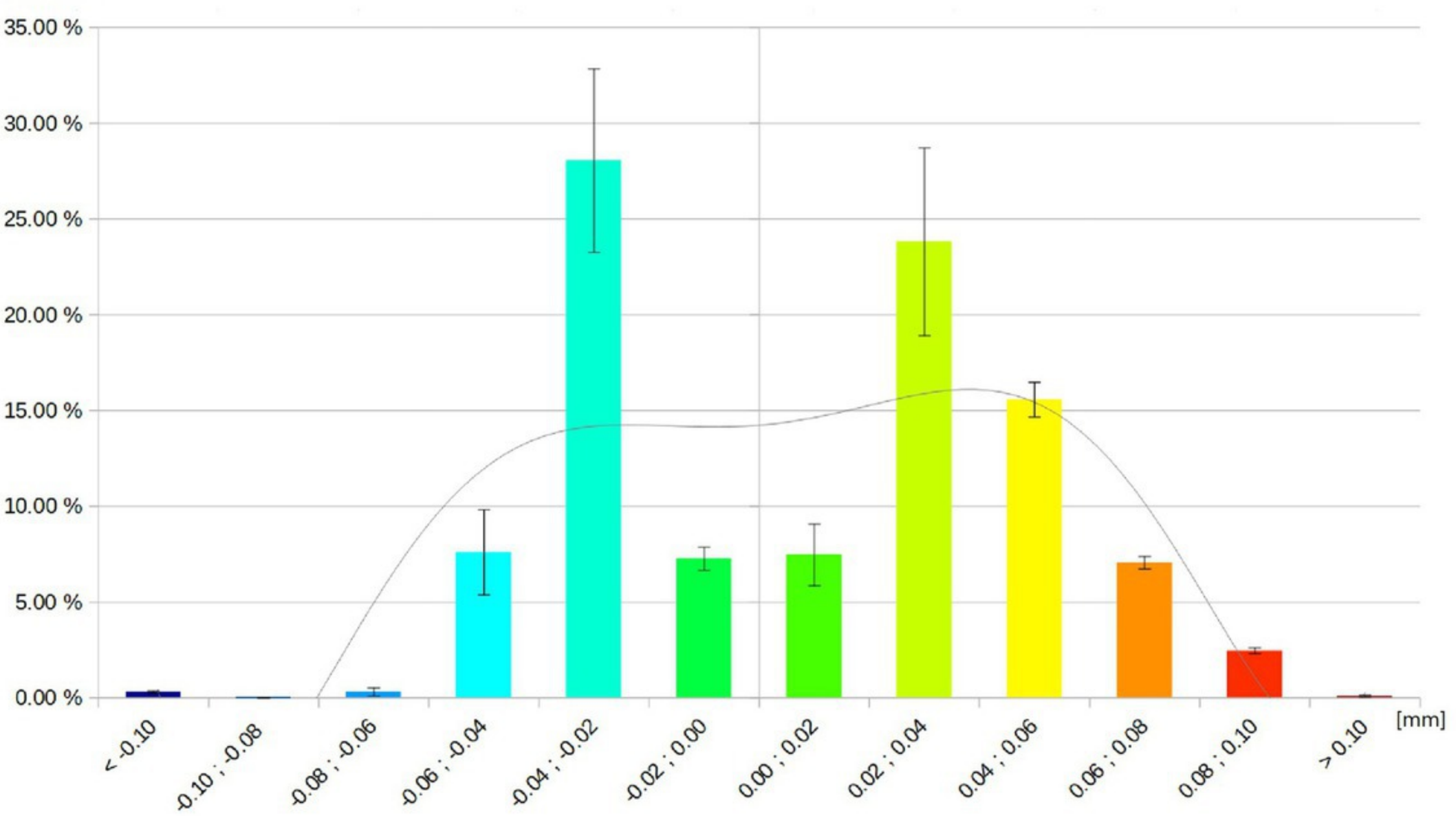
Tetric CAD



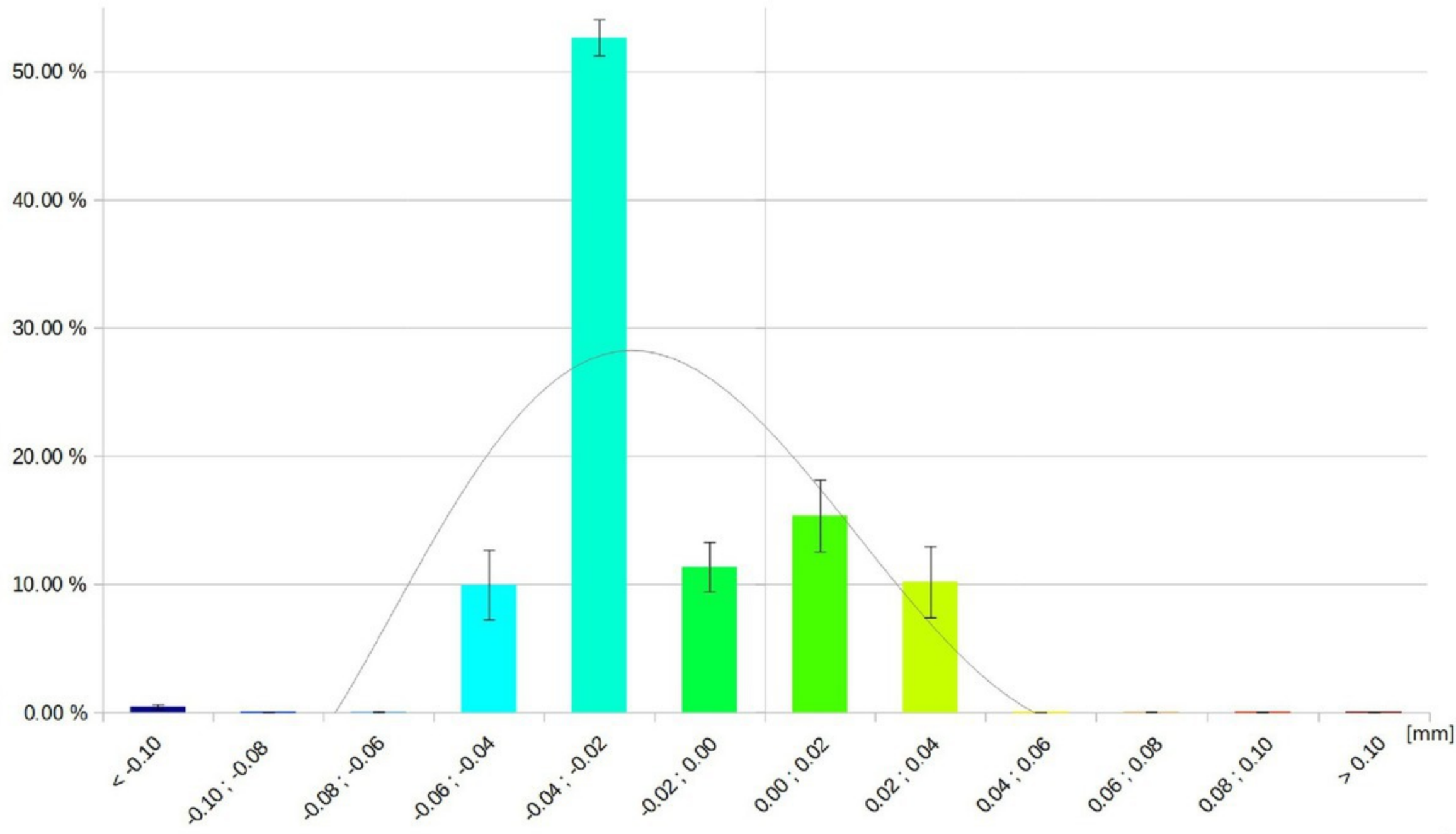
Empress CAD



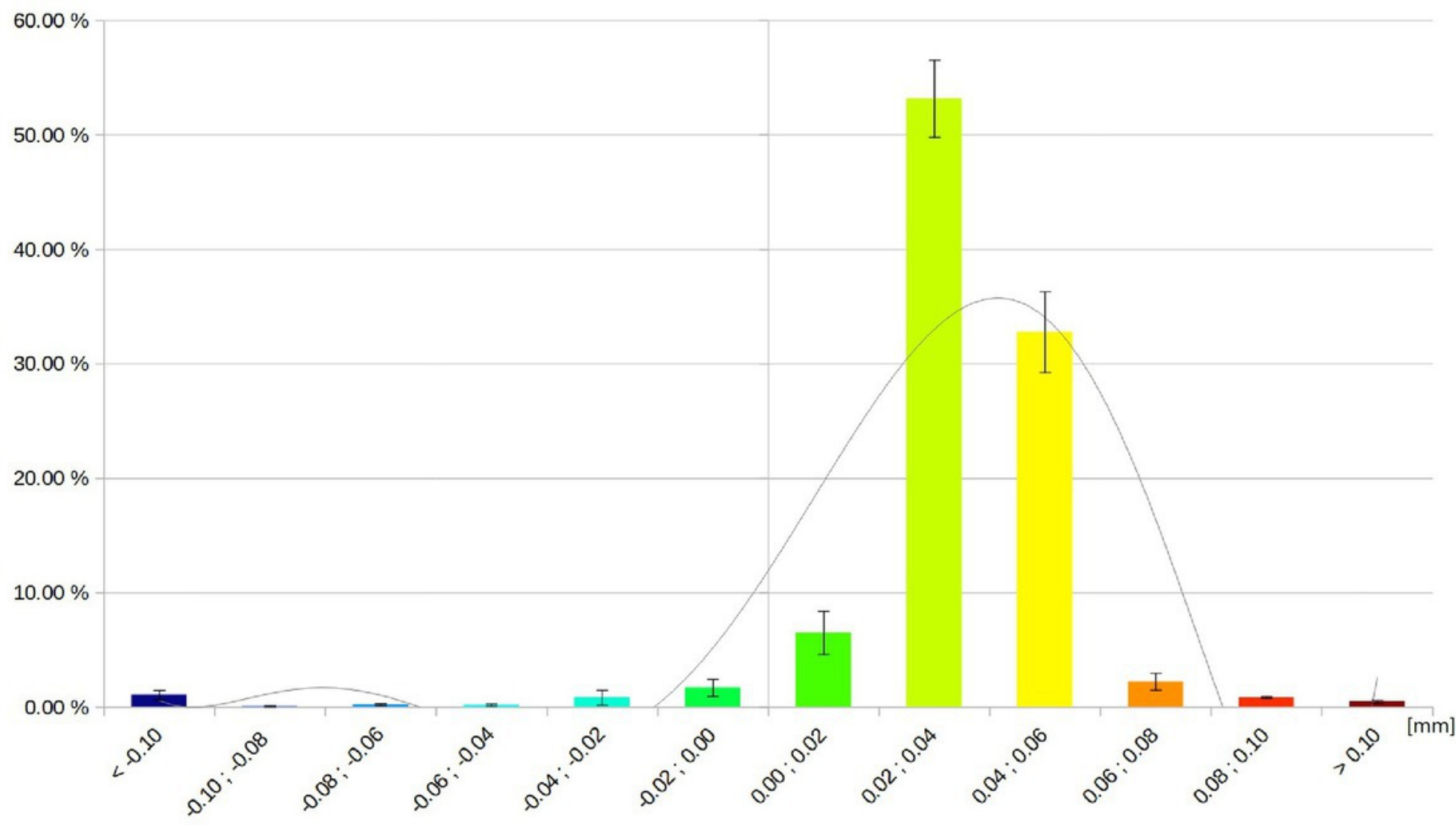
e.max CAD



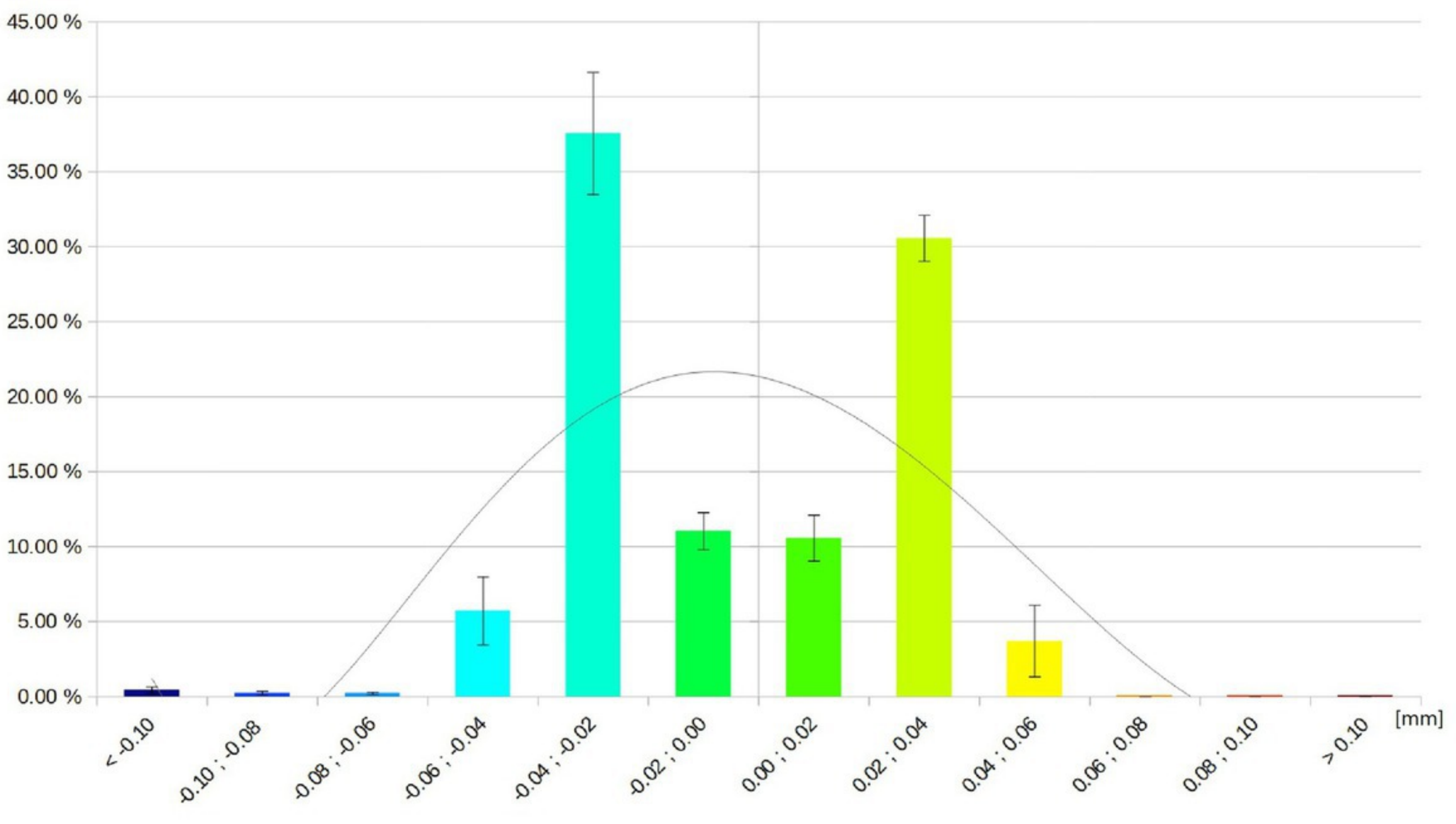
Tetric CAD



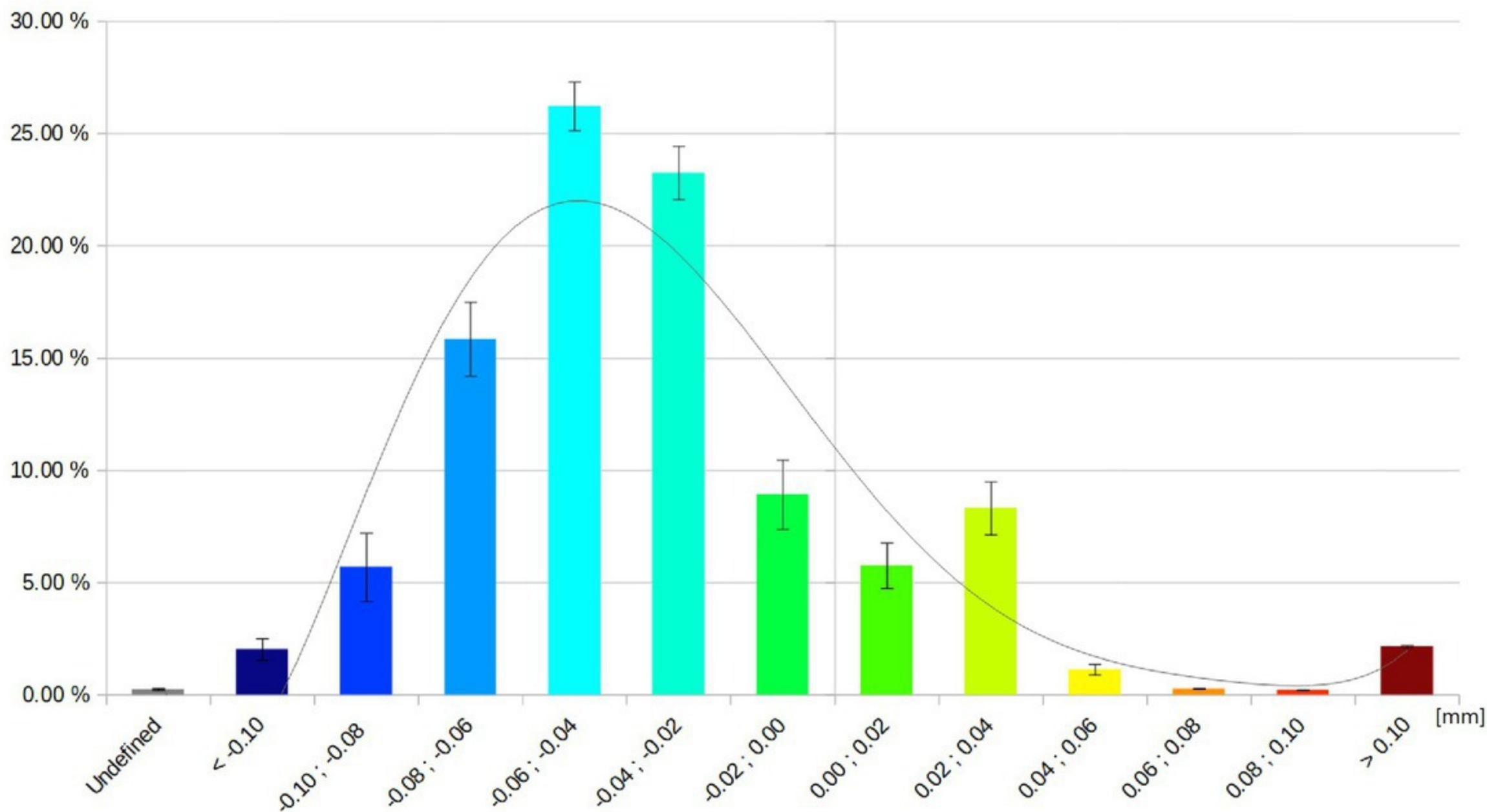
Empress CAD



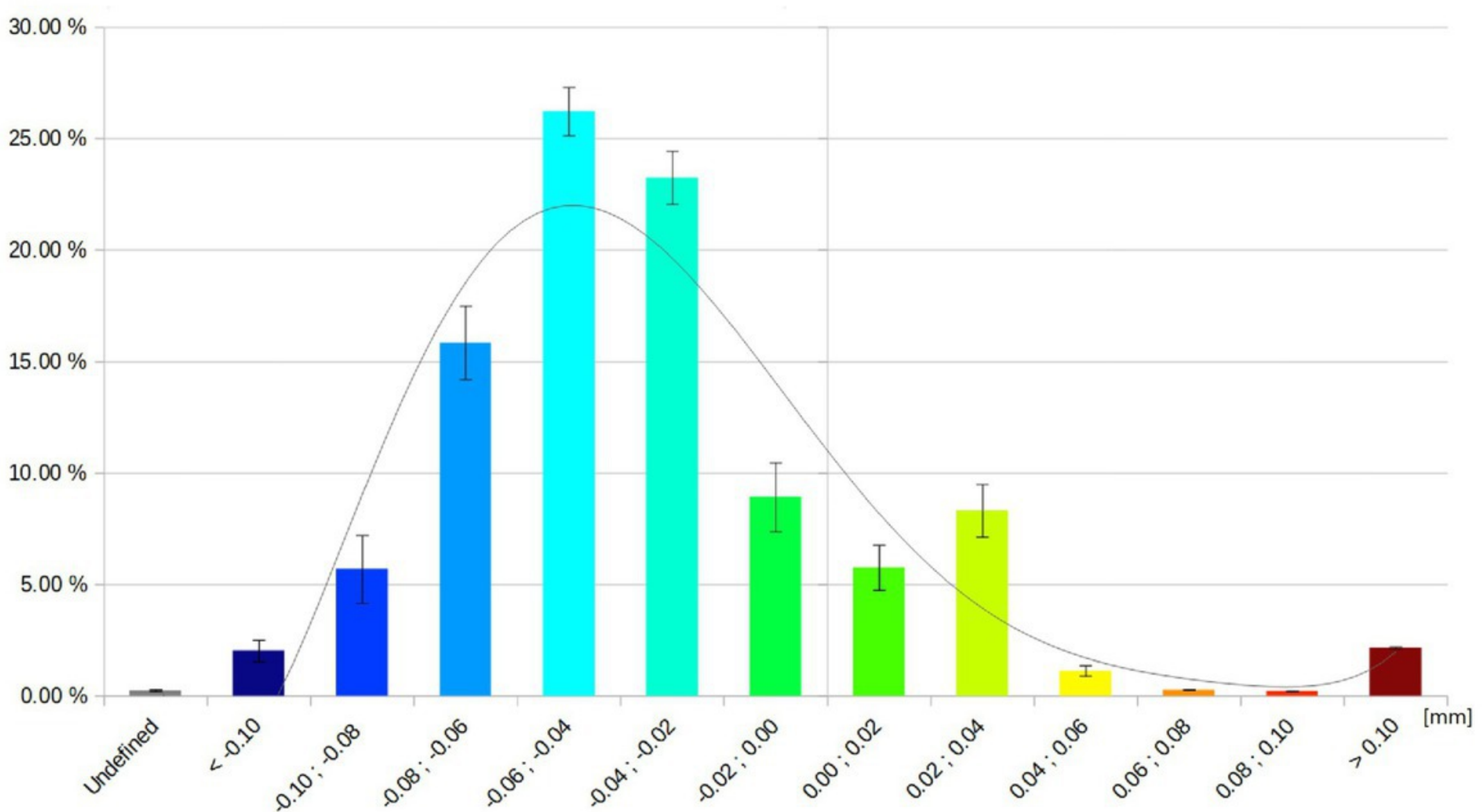
e.max CAD



Tetric CAD



Empress CAD



e.max CAD

